ACS Macro Letters

Letter

pubs.acs.org/macroletters

Nanopatterning Biomolecules by Block Copolymer Self-Assembly

Kato L. Killops,[†] Nalini Gupta,[‡] Michael D. Dimitriou,[†] Nathaniel A. Lynd,[†] Hyunjung Jung,[§] Helen Tran,[‡] Joona Bang,[§] and Luis M. Campos*[,‡]

[†]Materials Research Laboratory, Materials Department, and Department of Chemistry & Biochemistry, University of California, Santa Barbara, California 93106, United States

[‡]Department of Chemistry, Columbia University, New York, New York 10027, United States

[§]Department of Chemical and Biological Engineering, Korea University, 136-713 Seoul, Republic of Korea

Supporting Information

ABSTRACT: The fabrication of sub-100 nm features with bioactive molecules is a laborious and expensive process. To overcome these limitations, we present a modular strategy to create nanostructured substrates (ca. 25 nm features) using functional block copolymers (BCPs) based on poly(styrene-*b*-ethylene oxide) to controllably promote or inhibit cell adhesion. A single type of BCP was functionalized with a peptide, a perfluorinated moiety, and both compounds, to tune nanoscale phase separation and interactions with NIH3T3 fibroblast cells. The focal adhesion formation and morphology of the cells were observed to vary dramatically according to the functionality presented on the surface of the synthetic substrate. It is envisioned that these materials will be useful as substrates that mimic the extracellular matrix (ECM) given that the adhesion receptors of cells can recognize clustered motifs as small as 10 nm, and their spatial orientation can influence cellular responses.

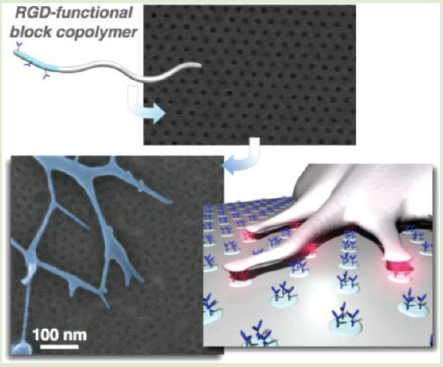

A number of important cellular processes originate from interactions with the dynamic and complex environment outside the cell, specifically, the extracellular matrix (ECM). Among the many interactions with the ECM, the adhesion receptors of cells can recognize clustered motifs as small as 10 nm, and their spatial orientation can dictate cell fate. One of the primary cellular interactions with the ECM is the formation of focal adhesions, which affects cell behavior including attachment, signaling, spreading, proliferation, and differentiation.[1,2] The peptide sequence of arginine-glycine-aspartic acid (RGD) has been identified as a minimal peptide binding sequence that is common to many ECM adhesive proteins including fibronectin, laminin, and collagen.[3] Presenting RGD ligands on the surface of synthetic biomimetic cell scaffolds yields a strategy to induce cell binding to the substrate and provide a means to study the diverse cellular processes resulting from focal adhesion formation. Non-patterned substrates coated with RGD randomly distributed on the surface has afforded information on the minimum surface concentration of ligands required for cell attachment,[4,5] whereas elegantly designed nanopatterned substrates by the groups of Spatz and Cooper-White have elucidated how cell binding and vitality are affected by integrin/ligand spacing.[6−8] Since the integrin proteins involved in focal adhesion formation have a diameter of 8−12 nm,[9,10] accessing this size regime is of utmost importance for studying the intricacies of cell−substrate contact.

Block copolymer (BCP) self-assembly is an emerging technology that has great potential in the microelectronics industry to create nanoscopic structures for next generation devices.[11] BCPs offer a wealth of versatility to create nanostructured patterns on surfaces with features ranging from 5 to 200 nm, which can be tuned by varying the molecular weight, architecture, and supramolecular interactions.[12] An added feature is that processing these materials is inexpensive, as compared to advanced lithographic techniques designed for sub-50 nm resolution.[13−15] While most of the advances in nanofabrication have been driven by miniaturization of semiconductors,[16] the patterning of (bio)molecules to interface with living organisms has been demonstrated to have tremendous impact in biotechnology,[17] where predicting and controlling cellular behavior through interactions with the ECM is of paramount concern.[18,19]

Nanoscale features, patterns, and topography between 10 and 60 nm have been shown to elicit dramatic responses from cells *in vitro*, even when the nature of the two-dimensional substrate is widely varied.[20−23] Creating and probing well-defined nanoscale features and interactions using conventional lithographic techniques, however, is time-consuming and difficult to achieve.[17,24,25] Often, expensive, highly specialized equipment is required, and the ability to achieve conformal coatings over large areas is limited. Herein, we present a method employing the self-assembly of functionalized BCPs[11] to obtain precisely defined, large-area nanopatterned scaffolds having tunable chemical functionality for cell cultures.

Received: March 28, 2012
Accepted: May 30, 2012
Published: June 5, 2012

   dx.doi.org/10.1021/mz300153k | *ACS Macro Lett.* 2012, 1, 758−763

Creating nanoscale domains through BCP lithography provides access to the size regime of integrins, which is crucial for elucidating the subtleties of focal contact formation.[19] Nanopatterns derived from phase separation of polystyrene-*b*-poly(4-vinylpyridine) exhibiting "dot-like" and "worm-like" domains were used by Hutmacher and co-workers to evaluate the adhesion and proliferation of cells on the synthetic substrates.[26] It was shown that the two cell types adhered and proliferated better on the worm-like surface, presumably due to the increased adsorption serum proteins leading to a more even coating on the lamellar material. Additionally, Glass et al. cleverly used the self-assembly of polystyrene-*b*-poly(2-vinylpyridine) micelles[27] to orient gold nanoparticles in a hexagonal array on surfaces, which have been used to probe cell adhesion phenomena and covalently anchor biomolecules to the synthetic surface.[6] By orienting RGD-binding motifs in a regularly spaced pattern, a number of variables affecting cell adhesion were probed, including RGD-ligand density, spacing, and alignment. However, the preparation of these substrates requires many steps,[27] and the use of electron beam lithography makes the patterning process expensive and precludes large scale production and multiplexing.[28] Furthermore, the full potential to employ BCPs for their exquisite ability to adopt a variety of morphological nanostructures remains to be exploited.[11,29]

To overcome the many issues associated with the nanopatterning of biomolecules, we have developed a modular BCP system that can be readily functionalized and easily processed to obtain reproducible biofunctional nanostructured substrates with large-area coverage. Recognizing that cell adhesion is mediated by a number of different parameters,[30,31] the modular nature of the approach presented here has enabled the synthesis of BCPs with vastly different properties, thus opening venues to explore molecular and geometric factors at the nanoscale that affect cellular functions. Considering the functional design of BCPs, it is widely known that their nanoscale self-assembly is affected by structural modifications at the molecular level. Both polymer end-group and backbone functionality have stark effects on self-assembly, especially with charged motifs,[32] hydrogen-bonding units,[33] and peptides,[34] among other moieties. BCPs of polystyrene-*b*-poly(ethylene oxide), PS-*b*-PEO, have been widely studied for their ability to form self-assembled nanostructured thin films under mild conditions (solvent annealing at room temperature),[35] but little is known about their assembly when the backbone of the PEO is functionalized with small, complex molecules, such as oligopeptides. Thus, this study presents a modular strategy to functionalize the PEO backbone with cell-adhesive peptides and other molecules to control the self-assembly of PS-*b*-PEO derivatives, and we demonstrate that the nanostructured features can be used for targeted cell adhesion. Importantly, we demonstrate the ability to tune the self-assembly of these materials by simply modifying a handful of functional units along the backbone, which in turn is an important factor for the overall performance of the BCPs under cell culture conditions. Scheme 1 depicts a peptide functional BCP specifically designed with a volume fraction composition that will lead to peptide-rich cylindrical domains immediately after processing, as opposed to postfunctionalization strategies where the amount of peptide incorporated can vary.[36,37] Therefore, it is expected that cells seeded on these thin-films will bind exclusively to the nanostructured features to enhance focal adhesion formation.

Scheme 1. Illustration of the Use of Functional Block Copolymer Thin Films as Substrates for Cell Culture

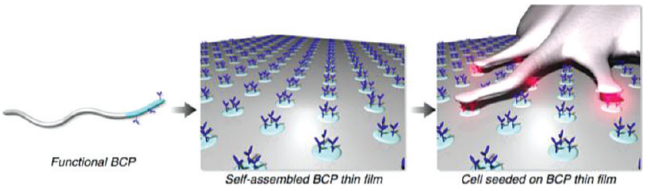

A BCP derivative of the PS-*b*-PEO system was chosen because its architecture can be designed to yield a nanophase-separated morphology, which matches the size regime of nanoscale integrins interacting with their environment.[2] The parent alkene-functional BCP (e-BCP, Figure 1a) is polystyrene-*b*-poly(ethylene oxide-*co*-allyl glycidyl ether) ($PS_{25.5K}$-*b*-$P[EO\text{-}co\text{-}AGE]_{11K}$, synthetic details found in the Supporting Information, SI).[38−40] By incorporating a small amount of AGE (3 mol %, relative to EO), the self-assembly properties of PS-*b*-PEO were expected to be preserved.[12] An advantage of this approach is that the allyl units can easily be covalently modified via the photochemical thiolene coupling reaction to afford functional BCPs incorporating a wide variety of chemical groups.[41−43] As a model system, a commercially available cysteine-modified peptide, Cys-Arg-Gly Asp-Ser (CRGDS),[44] was used to promote cell attachment.

To observe the effect of the AGE groups on the PEO backbone in e-BCP, thin films (ca. 40−60 nm thick) were prepared by spin coating onto glass slides and exposed to solvent annealing conditions to induce microphase segregation to obtain the nanostructured films. As observed in the atomic force microscope (AFM) image in Figure 1a, the resulting films display ordered hexagonal nanopatterns. To push the boundaries of the self-assembly of PEO-functional BCPs, the biomolecule of interest, CRGDS, was coupled to e-BCP to yield the peptide-functional material, pep-BCP. Upon spin coating on glass and solvent annealing, disordered, microphase segregated nanostructured coatings were observed (Figure 1b). The feature sizes were irregular and varied in size from 15 to 70 nm. The results were not surprising given the complexity of interactions that can arise from having multiple peptides with zwitterionic character along the hydrophilic portion of the BCP backbone. The morphology of these materials was studied by grazing-incidence small-angle X-ray scattering (GISAXS). GISAXS probes the nanostructure of the surface and interior of the thin films and can provide information on the size of microdomains and their preferential alignment relative to the surface. The parent system e-BCP exhibited cylinders oriented perpendicular to the substrate with a domain size of 33.5 nm, whereas the disordered pep-BCP film displayed an average *d*-spacing ca. 62 nm (Table S1 in the SI).

To improve the ordering of the peptide-functional materials, perfluorooctanethiol (PFOT) was used to modify interfacial interactions and to minimize nonspecific protein adsorption.[45,46] Fluorinated carbon chains generally do not mix with hydrophilic systems and many other hydrocarbons,[47] thereby serving as motifs to enhance phase segregation when bound to the hydrophilic domains. By varying the monomer feed ratio or reaction time for the first thiolene coupling with CRGDS, polymers with varying ratios of peptide to perfluoro groups can be subsequently synthesized using the parent polymer, such as the 1:1 peptide/PFOT functional BCP 1:1-BCP (Figure 1). In addition to the dual-functionalized material, a BCP containing

dx.doi.org/10.1021/mz300153k | *ACS Macro Lett.* 2012, 1, 758−763

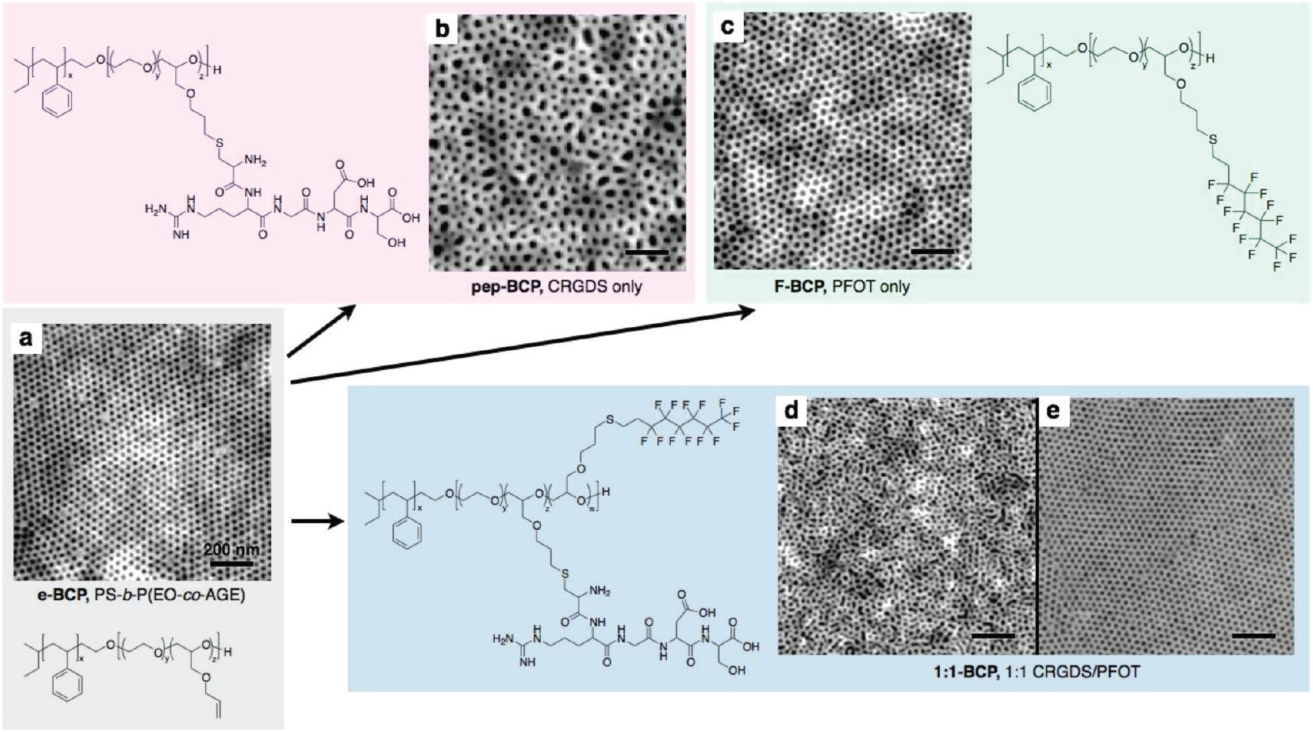

Figure 1. Chemical structures and height images from atomic force microscopy of block copolymer thin films. (a) Annealed film of e-BCP. (b) Annealed film of pep-BCP. (c) Annealed film of F-BCP. (d) As-cast film of 1:1-BCP. (e) Annealed film of 1:1-BCP. All scale bars are set to 200 nm. For the parent polymer and its derivatives, x = 245, y = 230, and z = 7. All scale bars represent 200 nm.

PFOT exclusively, F-BCP, was synthesized to gain a deeper understanding of the interplay between the factors that affect cell adhesion, repulsion, and BCP microphase segregation by comparing the functional groups in all BCPs.

Stark differences were observed upon modifying the small number (ca. 7 units) of functional groups on the backbone of the BCP (see the AFM images in Figure 1). The effect of fluorinated groups and peptides on the self-assembly behavior of functionalized PS-*b*-P(EO-*co*-AGE) copolymers is evident from the phase segregated structures. Interestingly, phase segregated films were obtained with 1:1-BCP, having a 1:1 ratio of peptide/PFOT along the PEO block (Figure 1d). These patterned substrates displayed nanotopography (Figure S4 in the SI), which has the potential to influence cell behavior.[23] However, our controls comparing the peptide-functional BCPs versus e-BCP show that the observed cell behavior arises from the presence of the peptide, not the topological features. Solvent annealing markedly improved the ordering (Figure 1e) to yield films of hexagonally packed cylinders with an average *d*-spacing ca. 26 nm confirmed by GISAXS (Table S1 in the SI). Control over the parallel or perpendicular orientation with respect to the substrate was achieved by simply varying the humidity of the annealing conditions (Figure S5 in the SI).[48] Its functionality and facile processing characteristics make 1:1-BCP a candidate for high-throughput applications with great potential to interface with biological systems. The PFOT-functional material F-BCP exhibits a uniform, hexagonally packed pattern (Figure 1c). The most dramatic change in the feature size was observed with F-BCP, having a *d*-spacing of 57.4 nm (Figure S3, Table S1 in the SI). The addition of perfluorinated groups into the PEO cylindrical domains prompted significant hydrophobic repulsion and an increase in the immiscibility between the blocks, inducing chain stretching leading to larger features.[49]

The polymer architecture was designed such that the peptides are localized in the PEO cylindrical domains. To demonstrate that the cells can access the peptide as depicted in Scheme 1, X-ray photoelectron spectroscopy (XPS) was used to characterize the elemental composition of functional groups at the surface of the films of the functionalized polymers. Films cast from polymers containing fluorine (1:1-BCP and F-BCP) display a characteristic strong binding energy peak at 689 eV (Figure S6 in the SI). As expected, pep-BCP containing only the CRGDS peptide does not exhibit a fluorine peak. However, a weak signal at 400 eV arising from the nitrogen electrons, exclusive to the peptide, is observed. A comparison of the spectra of pep-BCP and 1:1-BCP demonstrates that the peptide is present on the surface of both films to mediate cell adhesion (Figure S7 in the SI). Water contact angle measurements further support evidence of peptide being localized at the surface of the film (Table S2 in the SI), as both 1:1-BCP and pep-BCP exhibit angles ca. 60°.

Advantages of using this BCP system to evaluate cellular adhesion include its optical clarity and minimal thickness, permitting transmission of light through the sample, low autofluorescence, and the ability to create conformal nanostructured coatings over large areas. To serve as a model system in the evaluation of the adhesion-related properties of the synthetic matrices, NIH3T3 fibroblast cells were seeded onto the BCP-coated substrates and incubated for 24 h before fixing. The affinity of the cells for the nanoscale architecture and chemical composition of the substrates was evaluated with respect to cellular morphology and subcellular adhesive structures. To identify the dominant variables affecting cell adhesion, BCP substrates with varying incorporations of

dx.doi.org/10.1021/mz300153k | *ACS Macro Lett.* 2012, 1, 758−763

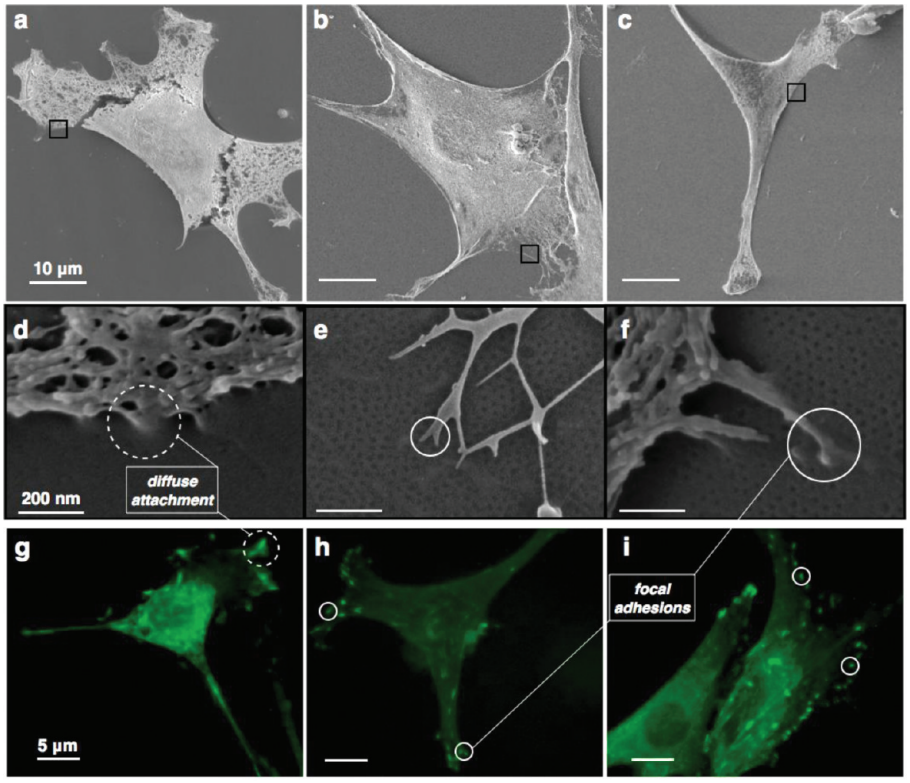

Figure 2. (a–f) SEM images of NIH3T3 cells seeded on polymer-coated substrates. (d–f) SEM images of magnified areas shown within boxes of (a–c) (enhanced to show contrast, original Figure S8 in SI). (g–i) Optical micrographs of NIH3T3 cells stained for vinculin. (a, d, g) PS control, (b, e, h) 1:1-BCP as-cast, (c, f, i), 1:1-BCP annealed. The focal adhesion sites are circled for clarity in figures h and i, whereas the filopodia are highlighted in parts e and f. Scale bars for a–c = 10 μm, d–f = 200 nm, g–i = 5 μm.

peptide and fluorinated groups were assessed, in addition to nonfunctionalized control substrates. The bright field microscope images of the cells seeded on polymer-coated glass substrates show dramatic differences in their morphology. Cells adhered to e-BCP, pep-BCP, 1:1-BCP, and PS (Figure 2 and Figures S8 and S9 in the SI) are large and well-spread. However, cells seeded on F-BCP (Figures S8a, iv and S9c in the SI) are substantially smaller and form clusters with other cells, rather than attaching and spreading onto the fluorinated polymer surface, indicating an unfavorable environment for cell binding.

The subcellular structures associated with forming focal adhesions were evaluated by staining adhered cells for vinculin (Figure 2 and Figure S8 in the SI).[50] Visual inspection of cells seeded on 1:1-BCP reveals that many focal adhesions appear at the periphery of the cell, indicated by bright, punctate spots (Figure 2h,i). These structures are accompanied by robust actin filaments, which are visualized by staining with phalloidin (Figure S8 in the SI). As previously reported by Kato et al.,[51] cells displaying a higher number of smaller focal adhesions were shown to have a higher affinity for the substrate than those with fewer adhesive aggregates. Furthermore, the colocalization of vinculin and actin has important implications for the connection of the cytoskeleton to the ECM, as well as for the signaling pathways that regulate cell growth.[2] Cells plated on the as-cast phase-separated 1:1-BCP also displayed many small, discrete focal adhesions (Figure 2i) and actin filaments spanning tens of micrometers (Figure S8 in the SI). Average cell areas were measured (Figure S10 in the SI), and except for cells plated on F-BCP, the cell areas were similar across all samples. Differences were observed, however, in the average number of vinculin plaques expressed by the cells (Figure S10 in the SI). Cells adhered to 1:1-BCP had significantly more discrete focal adhesions than all other substrates. Cells plated on PS displayed the lowest number of focal adhesions, and those that were observed were diffuse and not associated with actin filaments. The fact that cells display attachment behavior on the as-cast and annealed films of 1:1-BCP indicates the cytocompatibility of these materials and suggests that they can be employed to further understand the effect of nanostructured ECM mimics on cellular behavior.

To visualize the fine structural features of the cells that cannot be resolved by optical microscopy, the cells were dried using supercritical CO_2 and imaged by scanning electron microscopy (SEM). The typical cellular adhesive structures found on the PS control (a, d), dual-functionalized 1:1-BCP, annealed (b, e), and as-cast (c, f) films are shown in Figure 2. Cells adhered to the PS control do not exhibit individual locally adhered filopodial extensions (Figure 2d). On the other hand, sub-50 nm filopodial structures that extend from the periphery of the cells are clearly noticeable when the cells are adhered to substrates coated with 1:1-BCP. These structures were observed to specifically interact with the nanodomains on the surface, which correspond to the peptide-containing PEO. These structures are known to provide an exploratory function of the substratum environment surrounding the cell.[52] Notably, the conditions required to prepare a cell sample for SEM are quite harsh, and only the most robust peripheral cellular structures persist through electron microscopy imaging, indicating that the filopodia imaged on 1:1-BCP must be firmly adhered to the substrate. Observations of filopodial structures extending from cells adhered to the as-cast substrate

dx.doi.org/10.1021/mz300153k | ACS Macro Lett. 2012, 1, 758–763

(Figure 2f) indicate that these nanophase-separated coatings produced directly from spin coating are suitable for further studies of nanoscale focal adhesion formation in multiple cell types.

The focal adhesions arising from the three control materials shown (pep-BCP, e-BCP, and PS, Figure S8 and S9 in the SI, and Figure 2g, respectively) are fewer and more diffuse. Furthermore, the actin filaments are less pronounced and lack distinguishable organization in each of the controls. The formation of actin stress fibers and focal adhesions is related to cell migration and adhesion strength,[53] where small, punctate focal adhesions are indicative of motile cells and larger, elongated focal adhesions are associated with mature contacts with the ECM.[54] From these data, evidence for the interplay between the nanostructured surface and ligand display of the substrate emerges. With the exception of the PS control, each of the substrates displayed nanotopographical features (Figure S4 in the SI), the dominant factor in dictating stable focal adhesion formation, evaluated by staining, is the surface chemistry displayed to the cells. Although pep-BCP and 1:1-BCP both contain the cell adhesive peptide, the behavior of adherent cells on each is markedly different. To observe the thin-film behavior when immersed in solution, annealed films of pep-BCP and 1:1-BCP were swelled in cell growth media overnight before imaging by AFM in water. It was observed that pep-BCP swelled and the pattern deformed along the polyether domains after prolonged exposure to media, due to the hydrophilic nature of the PEO and the functional peptide (Figure 3b). However, Figure 3a shows that the 1:1-BCP

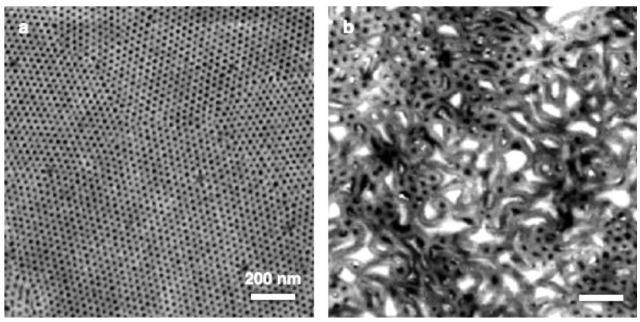

Figure 3. AFM height images of glass substrates coated with part a, annealed 1:1-BCP, and part b, annealed pep-BCP, imaged in water. Both substrates were submerged in cell growth media for 24 h prior to imaging.

nanostructured pattern remained intact. It can be inferred that the incorporation of the hydrophobic fluorinated chains in 1:1-BCP is required to preserve the ordered nanostructure under cell culture conditions, even after prolonged immersion in water.[55] For long-term cultures, the deformations observed from pep-BCP could have an effect on the ability of the cells to form stable focal adhesions[52] due to its dynamic swelling behavior and loss of pattern fidelity, as shown in Figure 3b.

In conclusion, a modular BCP system has been presented that affords nanoscale features accessed by self-assembly to target length scales of cellular focal adhesion sites. Modifying a small number of units along one of the blocks using molecules that exhibit strong interactions prompted drastic changes in the self-assembly of BCPs. However, appropriate modifications led to controlled phase segregation to obtain stable patterned films, even after prolonged exposure to cell media (1:1-BCP). Peptide and perfluorinated moieties were readily incorporated into the backbone of the parent polymer PS-*b*-P(EO-*co*-AGE) via thiolene click chemistry. It was observed that the domain sizes in the polymer thin films could be adjusted by changing the type and amount of functional group incorporation in the polyether domain. The incorporation of both CRGDS and PFOT in equal amounts into a polymer backbone was shown to promote focal adhesion formation with fine filopodial structures extending from the cell membrane, while maintaining the integrity of the patterned film under cell culture conditions. This material gave rise to nanostructured films directly after spin coating and ordered hexagonally packed cylinders after solvent annealing. The availability of nanoscale features afforded by BCP lithography with simple processing demonstrates a major advance in the production of nanostructured substrates for the study of cell adhesion phenomena. These materials and strategies enable precise control over nanoscale features as well as chemistries presented to the cell can open up venues for the mechanistic elucidation of cellular−substrate interactions.

■ ASSOCIATED CONTENT

Ⓢ Supporting Information

Materials, instrumentation, experimental details, and additional data. This material is available free of charge via the Internet at http://pubs.acs.org.

■ AUTHOR INFORMATION

Corresponding Author

*E-mail: lcampos@columbia.edu.

Notes

The authors declare no competing financial interest.

■ ACKNOWLEDGMENTS

This work made use of the MRL Central Facilities supported by the MRSEC Program of the National Science Foundation under award No. DMR05-20415, and we express our sincerest thanks to Craig J. Hawker (UCSB) for his open-hearted support and for providing us with resources. We thank Columbia University for start-up funds. K.L.K. thanks the DoD for a Science, Mathematics, and Research for Transformation (SMART) Fellowship. H.T. thanks the Department of Defense for an NDSEG Fellowship. H.J. and J.B. acknowledge the support by the Human Resources Development Program of KETEP grant (No. 20114010203050) and also by a Korea University Grant. We also thank Dr. Se Gyu Jang for the graphics shown in Figure 1.

■ REFERENCES

(1) Wozniak, M. A.; Modzelewska, K.; Kwong, L.; Keely, P. J. *Biochim. Biophys. Acta, Mol. Cell Res.* **2004**, *1692*, 103.
(2) Geiger, B.; Spatz, J. P.; Bershadsky, A. D. *Nat. Rev. Mol. Cell Biol.* **2009**, *10*, 21.
(3) Ruoslahti, E.; Pierschbacher, M. D. *Science* **1987**, *238*, 491.
(4) Massia, S. P.; Hubbell, J. A. *J. Cell. Biol.* **1991**, *114*, 1089.
(5) Maheshwari, G.; Brown, G.; Lauffenburger, D. A.; Wells, A.; Griffith, L. G. *J. Cell Sci.* **2000**, *113*, 1677.
(6) Arnold, M.; Cavalcanti-Adam, E. A.; Glass, R.; Blümmel, J.; Eck, W.; Kantlehner, M.; Kessler, H.; Spatz, J. P. *ChemPhysChem* **2004**, *5*, 383.
(7) Arnold, M.; Hirschfeld-Warneken, V.; Lohmüller, T.; Heil, P.; Blummel, J.; Cavalcanti-Adam, E. A.; López-García, M.; Walther, P.; Kessler, H.; Geiger, B.; Spatz, J. P. *Nano Lett.* **2008**, *8*, 2063.
(8) Frith, J. E.; Mills, R. J.; Cooper-White, J. J. *J. Cell Sci.* **2012**, *125*, 317.

(9) Erb, E.-M.; Tangemann, K.; Bohrmann, B.; Muller, B.; Engel, J. *Biochemistry* **1997**, *36*, 7395.
(10) Takagi, J.; Petre, B. M.; Walz, T.; Springer, T. A. *Cell* **2002**, *110*, 599.
(11) Bang, J.; Jeong, U.; Ryu, D. Y.; Russell, T. P.; Hawker, C. J. *Adv. Mater.* **2009**, *21*, 4769.
(12) Tang, C.; Lennon, E. M.; Fredrickson, G. H.; Kramer, E. J.; Hawker, C. J. *Science* **2008**, *322*, 429.
(13) Menard, E.; Meitl, M. A.; Sun, Y.; Park, J. U.; Shir, D. J. L.; Nam, Y. S.; Jeon, S.; Rogers, J. A. *Chem. Rev.* **2007**, *107*, 1117.
(14) Kolodziej, C. M.; Kim, S. H.; Broyer, R. M.; Saxer, S. S.; Decker, C. G.; Maynard, H. D. *J. Am. Chem. Soc.* **2012**, *134*, 247.
(15) Kolodziej, C. M.; Maynard, H. D. *Chem. Mater.* **2012**, *24*, 774−780.
(16) Black, C. T.; Ruiz, R.; Breyta, G.; Cheng, J. Y.; Colburn, M. E.; Guarini, K. W.; Kim, H. C.; Zhang, Y. *IBM J. Res. Dev.* **2007**, *51*, 605.
(17) Christman, K. L.; Enriquez-Rios, V. D.; Maynard, H. D. *Soft Matter* **2006**, *2*, 928.
(18) Tirrell, M.; Kokkoli, E.; Biesalski, M. *Surf. Sci.* **2002**, *500*, 61.
(19) Schmidt, R. C.; Healy, K. E. *J. Biomed. Mater. Res.* **2009**, *90A*, 1252.
(20) Park, J.; Bauer, S.; von der Mark, K.; Schmuki, P. *Nano Lett.* **2007**, *7*, 1686.
(21) Lim, J. Y.; Donahue, H. J. *Tissue Eng.* **2007**, *13*, 1879.
(22) Tay, C. Y.; Irvine, S. A.; Boey, F. Y. C.; Tan, L. P.; Venkatraman, S. *Small* **2011**, *7*, 1361.
(23) Dalby, M.; Riehle, M.; Johnstone, H.; Affrossman, S.; Curtis, A. *Biomaterials* **2002**, *23*, 2945.
(24) Kim, D.-H.; Lee, H.; Lee, Y.; Nam, J.-M.; Levchenko, A. *Adv. Mater.* **2010**, *22*, 4551.
(25) Schvartzman, M.; Palma, M.; Sable, J.; Abramson, J.; Hu, X.; Sheetz, M. P.; Wind, S. J. *Nano Lett.* **2011**, *11*, 1306.
(26) Khor, H. L.; Kuan, Y.; Kukula, H.; Tamada, K.; Knoll, W.; Moeller, M.; Hutmacher, D. W. *Biomacromolecules* **2007**, *8*, 1530.
(27) Glass, R.; Arnold, M.; Blümmel, J.; Küller, A.; Möller, M.; Spatz, J. P. *Adv. Funct. Mater.* **2003**, *13*, 569.
(28) Arnold, M.; Schwieder, M.; Blümmel, J.; Cavalcanti-Adam, E. A.; López-Garcia, M.; Kessler, H.; Geiger, B.; Spatz, J. P. *Soft Matter* **2009**, *5*, 72.
(29) Bates, F.; Fredrickson, G. *Annu. Rev. Phys. Chem.* **1990**, *41*, 525.
(30) Stevens, M. M.; George, J. H. *Science* **2005**, *310*, 1135.
(31) Kim, M.-H.; Kino-Oka, M.; Taya, M. *Biotechnol. Adv.* **2010**, *28*, 7.
(32) Hunt, J. N.; Feldman, K. E.; Lynd, N. A.; Deek, J.; Campos, L. M.; Spruell, J. M.; Hernandez, B. M.; Kramer, E. J.; Hawker, C. J. *Adv. Mater.* **2011**, *23*, 2327.
(33) Feldman, K. E.; Kade, M. J.; de Greef, T. F. A.; Meijer, E. W.; Kramer, E. J.; Hawker, C. J. *Macromolecules* **2008**, *41*, 4694.
(34) Zhang, Z.; Lai, Y.; Yu, L.; Ding, J. *Biomaterials* **2010**, *31*, 7873.
(35) Kim, S.; Misner, M. J.; Russell, T. P. *Adv. Mater.* **2004**, *16*, 2119.
(36) Saha, K.; Keung, A. J.; Irwin, E. F.; Li, Y.; Little, L.; Schaffer, D. V.; Healy, K. E. *Biophys. J.* **2008**, *95*, 4426.
(37) George, P. A.; Doran, M. R.; Croll, T. I.; Munro, T. P.; Cooper-White, J. J. *Biomaterials* **2009**, *30*, 4732.
(38) Lee, B. F.; Kade, M. J.; Chute, J. A.; Gupta, N.; Campos, L. M.; Fredrickson, G. H.; Kramer, E. J.; Lynd, N. A.; Hawker, C. J. *J. Polym. Sci., Part A: Polym. Chem.* **2011**, *49*, 4498.
(39) Hrubý, M.; Konak, C.; Ulbrich, K. *J. Appl. Polym. Sci.* **2005**, *95*, 201.
(40) Erberich, M.; Keul, H.; Möller, M. *Macromolecules* **2007**, *40*, 3070.
(41) Hoyle, C. E.; Bowman, C. N. *Angew. Chem., Int. Ed.* **2010**, *49*, 1540.
(42) Campos, L. M.; Killops, K. L.; Sakai, R.; Paulusse, J. M. J.; Damiron, D.; Drockenmuller, E.; Messmore, B. W.; Hawker, C. J. *Macromolecules* **2008**, *41*, 7063.
(43) Campos, L. M.; Truong, T. T.; Shim, D. E.; Dimitriou, M. D.; Shir, D.; Meinel, I.; Gerbec, J. A.; Hahn, H. T.; Rogers, J. A.; Hawker, C. J. *Chem. Mater.* **2009**, *21*, 5319.
(44) Gupta, N.; Lin, B.; Campos, L.; Dimitriou, M.; Hikita, S.; Treat, N.; Tirrell, M.; Clegg, D.; Kramer, E.; Hawker, C. *Nat. Chem.* **2009**, *2*, 138.
(45) Park, D.; Weinman, C. J.; Finlay, J. A.; Fletcher, B. R.; Paik, M. Y.; Sundaram, H. S.; Dimitriou, M. D.; Sohn, K. E.; Callow, M. E.; Callow, J. A.; Handlin, D. L.; Willis, C. L.; Fischer, D. A.; Kramer, E. J.; Ober, C. K. *Langmuir* **2010**, *26*, 9772.
(46) Dimitriou, M. D.; Zhou, Z.; Yoo, H.-S.; Killops, K. L.; Finlay, J. A.; Cone, G.; Sundaram, H. S.; Lynd, N. A.; Barteau, K. P.; Campos, L. M.; Fischer, D. A.; Callow, M. E.; Callow, J. A.; Ober, C. K.; Hawker, C. J.; Kramer, E. J. *Langmuir* **2011**, *27*, 13762.
(47) Iyengar, D. R.; Perutz, S. M.; Dai, C. A.; Ober, C. K.; Kramer, E. J. *Macromolecules* **1996**, *29*, 1229.
(48) Bang, J.; Kim, B.; Stein, G.; Russell, T.; Li, X.; Wang, J.; Kramer, E.; Hawker, C. *Macromolecules* **2007**, *40*, 7019.
(49) Davidock, D. A.; Hillmyer, M. A.; Lodge, T. P. *Macromolecules* **2004**, *37*, 397.
(50) Humphries, J. D.; Wang, P.; Streuli, C.; Geiger, B.; Humphries, M. J.; Ballestrem, C. *J. Cell. Biol.* **2007**, *179*, 1043.
(51) Kato, M.; Mrksich, M. *Biochemistry* **2004**, *43*, 2699.
(52) Geiger, B.; Bershadsky, A.; Pankov, R.; Yamada, K. M. *Nat. Rev. Mol. Cell Biol.* **2001**, *2*, 793.
(53) Balaban, N. Q.; Schwarz, U.; Riveline, D.; Goichberg, P.; Tzur, G.; Sabanay, I.; Mahalu, D.; Safran, S.; Bershadsky, A.; Addadi, L.; Geiger, B. *Nat. Cell Biol.* **2001**, *3*, 466.
(54) Pelham, R. J.; Wang, Y. *Proc. Natl. Acad. Sci.* **1997**, *94*, 13661.
(55) Gudipati, C. S.; Finlay, J. A.; Callow, J. A.; Callow, M. E.; Wooley, K. L. *Langmuir* **2005**, *21*, 3044.